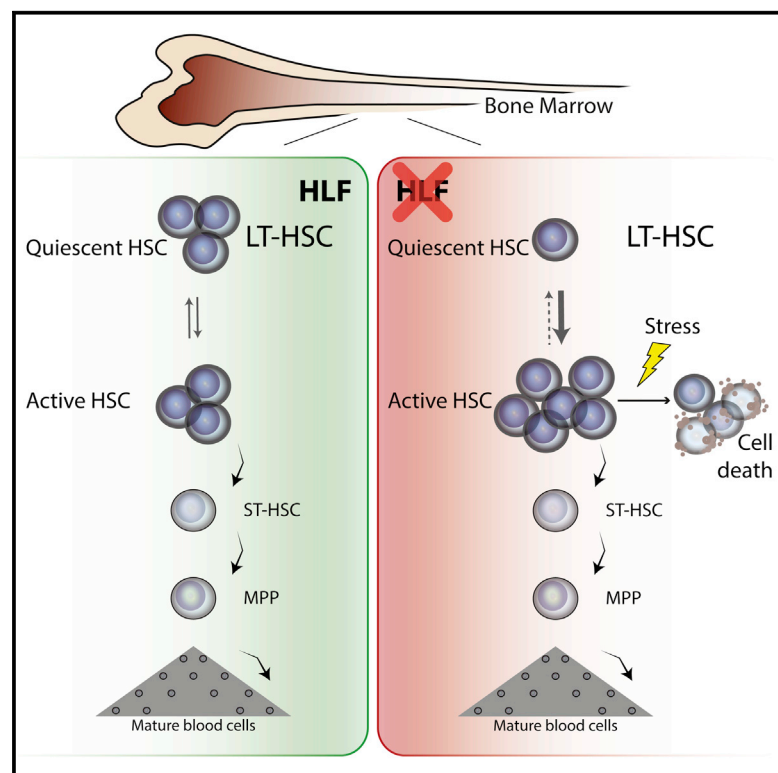


Hepatic Leukemia Factor Maintains Quiescence of Hematopoietic Stem Cells and Protects the Stem Cell Pool during Regeneration

Graphical Abstract



Authors

Karolina Komorowska, Alexander Doyle, Martin Wahlestedt, ..., David Bryder, Jonas Larsson, Mattias Magnusson

Correspondence

mattias.magnusson@med.lu.se

In Brief

Komorowska et al. report that the transcription factor HLF is required to maintain hematopoietic stem cell (HSC) function during regeneration. Moreover, *Hlf*-deficient HSCs are less quiescent. In accordance with this, toxic insults targeting dividing cells completely eradicate the HSC pool in *Hlf*-deficient mice.

Highlights

- HLF is dispensable for steady-state hematopoiesis
- HLF is required to maintain HSC function during serial repopulation
- HLF-deficient HSCs display loss of quiescence
- HSCs lacking HLF show increased sensitivity to chemotoxic insults

Data and Software Availability

GSE100385
GSE69817



Hepatic Leukemia Factor Maintains Quiescence of Hematopoietic Stem Cells and Protects the Stem Cell Pool during Regeneration

Karolina Komorowska,¹ Alexander Doyle,¹ Martin Wahlestedt,² Agatheeswaran Subramaniam,¹ Shubhranshu Debnath,¹ Jun Chen,¹ Shamit Soneji,² Ben Van Handel,^{3,4} Hanna K.A. Mikkola,⁵ Kenichi Miharada,¹ David Bryder,² Jonas Larsson,¹ and Mattias Magnusson^{1,6,*}

¹Molecular Medicine and Gene Therapy, Lund Stem Cell Center, Lund University, BMC A12, 221 84, Lund, Sweden

²Molecular Hematology, Lund Stem Cell Center, Lund University, BMC A12, 221 84, Lund, Sweden

³Department of Stem Cell Biology and Regenerative Medicine, Keck School of Medicine, University of Southern California, Los Angeles, CA 90033, USA

⁴CarthroniX, Inc., Tarzana, CA 91356, USA

⁵Department of Molecular, Cell and Developmental Biology, University of California, Los Angeles, Los Angeles, CA 90095, USA

⁶Lead Contact

*Correspondence: mattias.magnusson@med.lu.se

<https://doi.org/10.1016/j.celrep.2017.11.084>

SUMMARY

The transcription factor hepatic leukemia factor (HLF) is strongly expressed in hematopoietic stem cells (HSCs) and is thought to influence both HSC self-renewal and leukemogenesis. However, the physiological role of HLF in hematopoiesis and HSC function is unclear. Here, we report that mice lacking *Hlf* are viable with essentially normal hematopoietic parameters, including an intact HSC pool during steady-state hematopoiesis. In contrast, when challenged through transplantation, *Hlf*-deficient HSCs showed an impaired ability to reconstitute hematopoiesis and became gradually exhausted upon serial transplantation. Transcriptional profiling of *Hlf*-deficient HSCs revealed changes associated with enhanced cellular activation, and cell-cycle analysis demonstrated a significant reduction of quiescent HSCs. Accordingly, toxic insults targeting dividing cells completely eradicated the HSC pool in *Hlf*-deficient mice. In summary, our findings point to HLF as a critical regulator of HSC quiescence and as an essential factor for maintaining the HSC pool during regeneration.

INTRODUCTION

The maintenance of a functional and fully potent pool of hematopoietic stem cells (HSCs) is essential to sustain continuous blood production and enable recovery of the hematopoietic system after an insult (Bryder et al., 2006; Weissman, 2000). However, despite the enormous cellular turnover needed to ensure appropriate hematopoiesis, HSCs themselves are typically highly quiescent, which is a feature that offers protection against various types of stress-induced damage that can otherwise be caused by continuous replication and cellular respiration (Elias-

son and Jönsson, 2010). By contrast, HSCs can be rapidly mobilized to proliferate and reconstitute the hematopoietic system upon an insult. At a molecular level, these critical processes are regulated by defined transcription factors, and studies using genetically modified mice or translocations causing human leukemia have established transcription factor networks that critically influence HSC fate options (Orkin and Zon, 2008).

Hepatic leukemia factor (HLF), a member of the proline and acidic amino-acid-rich (PAR) basic leucine zipper (bZip) family, was originally identified as part of the t(17:19)(E2A-HLF) translocation, which underlies a rare subtype of pediatric acute lymphoblastic leukemia (ALL) (Inaba et al., 1992). In contrast to most ALL types, the E2A-HLF subtype is chemotherapy resistant and associated with high mortality, usually within 2 years of the diagnosis (Hunger et al., 1992; Inukai et al., 2007). In addition, more recent transcriptional profiling studies have implicated HLF as a “stemness” gene in both normal and malignant hematopoiesis (Dorn et al., 2009; Gazit et al., 2013; Ivanova et al., 2002; Magnusson et al., 2013; Moore et al., 2007; Shojaei et al., 2005), as HLF is highly expressed in the HSC pool and gradually downregulated upon differentiation (Gazit et al., 2013).

In hematopoiesis, ectopic expression of HLF alone was shown to increase engraftment of human cord blood cells and improve multi-lineage potential and self-renewal of HSC *in vitro* (Gazit et al., 2013; Shojaei et al., 2005). Moreover, Riddell et al. recently found HLF to be one of six transcription factors that together are capable of reprogramming B cells into HSC-like cells *in vivo* (Riddell et al., 2014). Thus, enforced expression of HLF is strongly associated with enhanced HSC activity in both humans and mice, yet whether endogenous HLF plays a physiological role in HSC regulation has not been assessed.

Here, using HLF-knockout mice, we show that HLF deficiency causes a gradual depletion of HSC activity during serial repopulation. Moreover, HLF-deficient HSCs display a loss of quiescence and show increased sensitivity to chemotoxic insult or irradiation. Our findings therefore depict an essential role for HLF in preserving HSC quiescence.



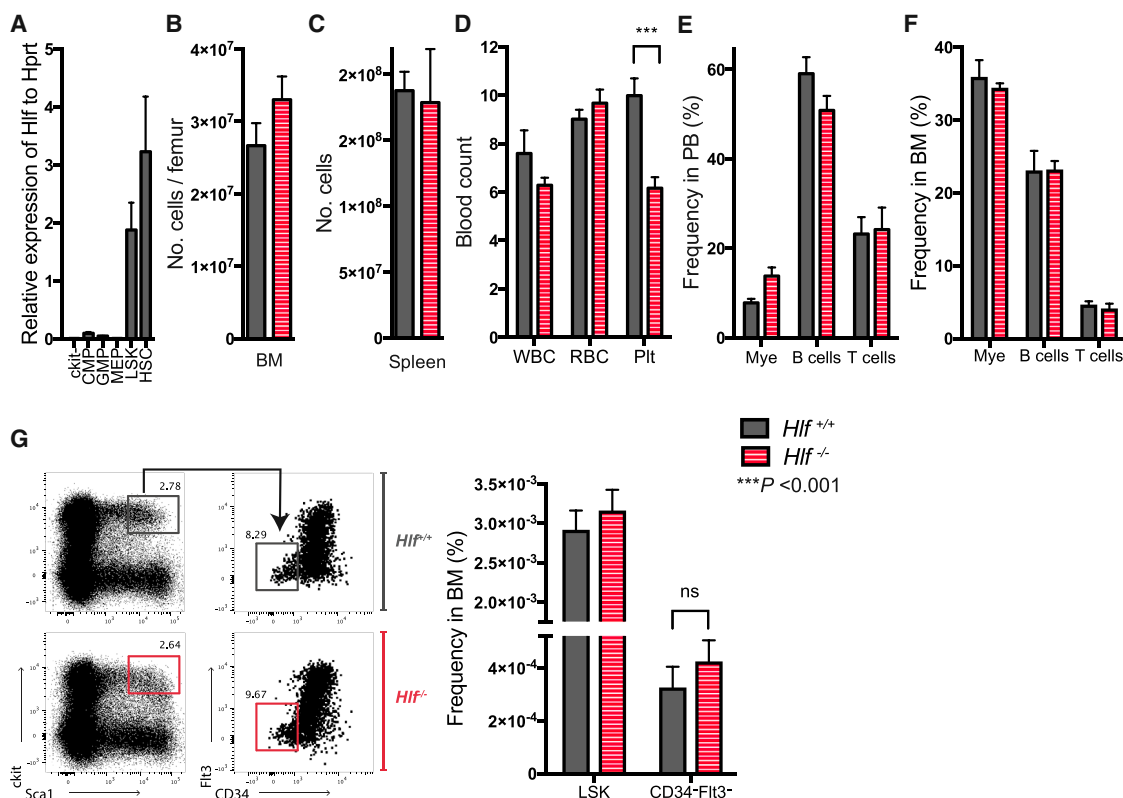


Figure 1. *Hlf*^{-/-} Mice Display Normal Blood Cell Parameters and Frequencies of Hematopoietic Stem and Progenitor Cells

(A) Relative levels of *Hlf* mRNA evaluated by real-time qPCR in comparison to *Hprt* in HSCs, LSKs, MEPs, GMPs, CMPs, and ckit⁺ cells isolated from WT mouse BM (n = 3).

(B and C) Total number of nucleated cells in (B) bone marrow (BM) and (C) spleen.

(D) White blood cell (WBC) counts (× 10⁹), red blood cell (RBC) counts (× 10¹²), and platelet (Plt) counts (× 10¹¹).

(E and F) Lineage distribution in peripheral blood (PB) (E) and BM (F) at steady-state hematopoiesis assessed by flow cytometry.

(G) Representative FACS plots of LSK and HSCs (LSK CD34⁻ Flt3⁻) from BM of 16-week-old *Hlf*^{+/+} and *Hlf*^{-/-} mice. Bars to the right display the frequency of LSK and HSCs in the BM from 10 mice.

All analyses were done using 4-month-old *Hlf*^{-/-} mice and *Hlf*^{+/+} littermate controls (n > 3 per genotype). Data represent mean values. Error bars represent SEM. The asterisks indicate significant differences (p).

RESULTS

HLF Is Dispensable for Steady-State Hematopoiesis

To investigate the physiological role of HLF in hematopoiesis, we first determined its expression pattern in isolated hematopoietic stem and progenitor cell populations from mouse bone marrow (BM) by real-time qPCR. The analysis showed that HLF is highly and preferentially expressed in HSCs and multipotent progenitors and less expressed in more committed progenitor populations (Figure 1A), consistent with previous transcriptome profiling studies (Gazit et al., 2013; Ivanova et al., 2002). Next, to assess the functional consequences of HLF deficiency on hematopoiesis, we employed a conventional knockout mouse model for *Hlf* (Gachon et al., 2004). The *Hlf*^{-/-} mice were fertile and born at a normal Mendelian ratio (data not shown). At 12–16 weeks of age, *Hlf*^{-/-} mice displayed normal body weight (data not shown), as well as normal cellularity of both BM and spleen (Figures 1B and 1C). Peripheral blood (PB) analysis revealed no significant changes in the blood cell counts of *Hlf*^{-/-} mice, with the exception of reduced platelet numbers (Figure 1D).

To investigate whether the observed bias in platelets is a result of perturbed differentiation capacity, we analyzed the early stages of megakaryopoiesis potential using flow cytometry. While the relative proportions of pre-MegE (common megakaryocyte/erythroid progenitor) and pre-CFU-E (erythroid restricted progenitor) cells were unchanged, we observed a significant reduction in phenotypic MkP (megakaryocyte restricted progenitor), suggesting that HLF deficiency results in a reduced differentiation capacity specifically toward platelets (Figure S1).

Additional evaluations by flow cytometry showed a normal frequency and distribution of mature blood cells in both PB and BM (Figures 1E and 1F). Taken together, these data show that mice can sustain essentially normal hematopoietic parameters in the absence of HLF.

Since HLF is mainly expressed in HSCs and their immediate downstream progeny, we next analyzed the BM in more detail to assess the frequency of Lin⁻Sca1⁺c-Kit⁺ (LSK) cells and LSK CD34⁻Flt3⁻ (HSC) cells. Surprisingly, no significant change was observed in the frequency of immunophenotypic stem/progenitor populations between the *Hlf*^{-/-} and littermate *Hlf*^{+/+}

control mice (Figure 1G). Overall, these findings suggest that HLF is dispensable for steady-state hematopoiesis under normal physiological conditions *in vivo*.

HLF-Deficient HSCs Have Reduced Serial Repopulating Capacity *In Vivo*

To analyze the functional role of HLF in HSC regulation under more challenging conditions, we next transplanted BM cells from *Hlf*^{-/-} or littermate *Hlf*^{+/+} control mice in a competitive setting (1:1 ratio) to test their regenerative potential (Figure 2A). PB analysis at 8 and 16 weeks post-transplantation showed a significant reduction in the donor contribution (chimerism) of the *Hlf*^{-/-} cells in comparison to *Hlf*^{+/+} cells (Figure 2B), although no change in lineage distribution was observed (Figures 2C and 2D). At 16 weeks post-transplantation, the BM of engrafted mice was analyzed. This revealed a similar reduction in the chimerism of *Hlf*^{-/-} HSC-derived cells as seen in the PB analysis (Figure 2E). Of note, the reduction was more pronounced in the LSK population that contains HSC and progenitor cells, indicating that the role of HLF is more important for immature cells (Figure 2E). To address whether HLF deficiency specifically impairs the self-renewal capacity of HSCs, BM cells from the primary recipients were serially transplanted to secondary and tertiary recipients (Figures 2F and 2G). BM analysis showed that the reduced reconstitution capacity seen in the primary recipients of the *Hlf*^{-/-} BM cells was even more pronounced in secondary recipients (Figure 2F), with dismal reconstitution detected in tertiary recipients (Figure 2G). This establishes that HSC activity is compromised during regenerative conditions in the absence of HLF.

To investigate whether the reduced long-term engraftment capacity is caused by an overall reduction of the HSC pool size, competitive repopulation units (CRUs) were quantified by transplanting limited doses of *Hlf*^{+/+} or *Hlf*^{-/-} BM in a competitive setting (Figure 2H). No changes in CRU frequencies were detected between *Hlf*^{-/-} and *Hlf*^{+/+} BM, demonstrating that the number of HSCs are not affected in *Hlf*^{-/-} mice.

To more directly establish that the long-term effect of HLF loss on hematopoiesis is a result of reduced HSC function, we competitively transplanted 50 purified HSCs (LSK CD34⁻Flt3⁻) from either *Hlf*^{-/-} or *Hlf*^{+/+} control mice (Figure 2I). Analysis at 16 weeks post-transplantation showed a reduction in reconstitution capacity similar to that seen in unfractionated BM (Figure 2J), strongly arguing for a reduced regenerative potential of *Hlf*^{-/-} HSCs on a per-cell basis. Taken together, the results of the transplantation experiments demonstrate that expression of HLF is crucial for HSCs to maintain their self-renewal potential during hematopoietic reconstitution.

Gene Expression and ChIP-Seq Analysis Suggest that HLF Regulates HSC Cell-Cycle Activity

Since previous findings have shown that overexpression of HLF results in a pro-survival effect (Shojaei et al., 2005; Waters et al., 2013), we asked whether the impaired reconstitution capacity of *Hlf*^{-/-} HSCs is due to increased apoptosis. However, evaluations of Annexin-V failed to reveal a significant difference in the frequency of apoptotic cells between *Hlf*^{-/-} and *Hlf*^{+/+} LSK cells (Figure 3A), implying the involvement of other mechanisms. To elucidate the molecular consequences of HLF loss in HSC regu-

lation, we next performed genome-wide expression analysis using RNA-seq of purified *Hlf*^{-/-} and *Hlf*^{+/+} HSCs (LSK CD34⁻Flt3⁻ cells). This revealed 550 differentially expressed genes (256 upregulated and 294 downregulated, *p* < 0.05, 1.5-fold cut off) (Table S1). Among the downregulated genes, we identified transcription factors known to be important for maintaining normal HSC activity (GFI1 and IRF2) (Hock et al., 2004; Sato et al., 2009), while among the upregulated genes, we identified several genes known to regulate cell-cycle activity (Table S2). By applying Gene Ontology (GO) analysis on the differentially expressed genes, we revealed a significant enrichment of cell cycle, DNA replication, and cellular stress response genes among the genes upregulated in *Hlf*^{-/-} HSCs (Figure 3B; Table S2).

Similarly, gene set enrichment analysis (GSEA) showed that the upregulated genes in *Hlf*^{-/-} HSCs were significantly associated with gene sets related to cell cycle and DNA replication (Figure 3C). In line with this, the transcriptome of the *Hlf*^{-/-} HSCs significantly correlated to the transcriptome of short-term HSCs (ST-HSCs) (a set of genes extracted that are known to be more mitotically active than long-term HSCs (LT-HSCs); Ficara et al., 2008) (Figures 3D and 3E).

To determine whether HLF directly binds to regulatory elements of genes regulating HSC activity, we obtained chromatin immunoprecipitation sequencing (ChIP-seq) data from mouse LSK cells overexpressing *Hlf* (Wahlestedt et al., 2017). The dataset identified 693 genes bound by HLF, with a binding motif similar to the known HLF-binding site described in Wahlestedt et al. (2017).

Intersection of the ChIP-seq data with the transcriptome data based on fold change, irrespective of the *q* value, revealed that more than 30% of HLF-bound genes (229 out of 693) were transcriptionally modulated in *Hlf*^{-/-} HSCs (Figure S2). This suggests that a substantial number of the modulated genes from the RNA sequencing (RNA-seq) analysis are direct targets of HLF. Among the overlapping genes, we observed two distinct clusters, one with upregulated and one with downregulated genes. This suggests that HLF may act both as an activator and a repressor in the HSC context. GO analysis of the overlapping genes revealed an enrichment of gene sets regulating cell activity and stress response among the upregulated genes, while the downregulated genes were enriched for transcriptional regulation (data not shown).

By overlapping ChIP targets with the significantly regulated genes, we identified a set of transcription factors that were all downregulated in *Hlf*^{-/-} HSCs (Figure 3F). Among these transcription factors, we found *Nfic* (identified as a direct target of HLF in Wahlestedt et al., 2017) and *Irf2*, which is an important regulator of HSC quiescence (Sato et al., 2009) (Figure 3F). When intersecting the HLF-binding data with ChIP-seq data of active histone marks in HSC and assay for transposase-accessible chromatin (ATAC) sequencing data in LSK cells (Wahlestedt et al., 2017), we could confirm that HLF directly binds to the promoter region (surrounded by active histone marks) as well as to possible enhancer regions of *Irf2* (Figure 3G). This suggests that HLF directly promotes the transcription of *Irf2* in HSCs.

Taken together, these data suggest that HLF is important in regulating HSC quiescence and that HLF may act as both a repressor and an activator of gene function in HSCs.

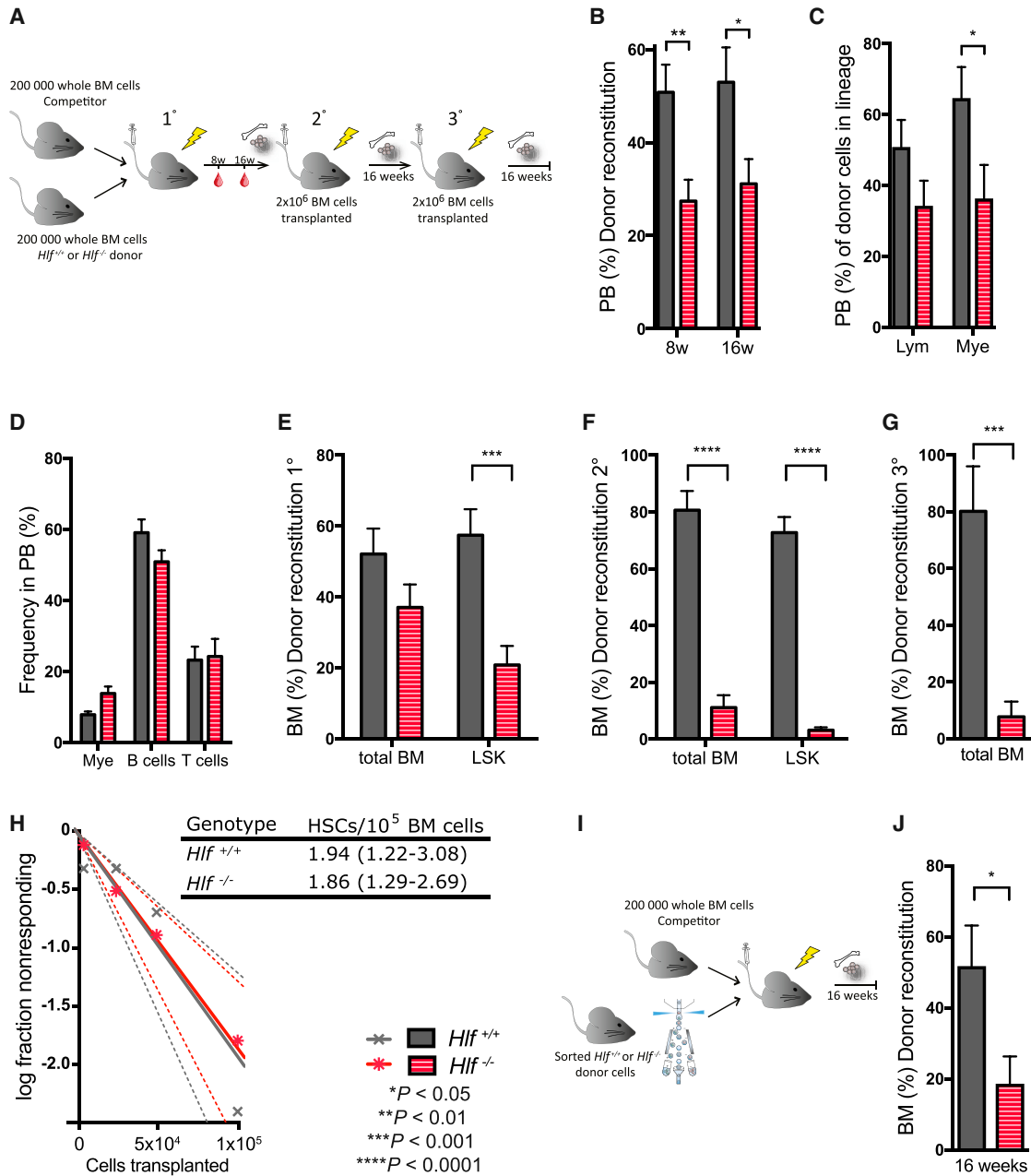


Figure 2. HLF-Deficient HSCs Have Reduced Serial Repopulating Capacity In Vivo

(A) Schematic overview of the competitive serial transplantation assay using whole BM from *Hlf*^{-/-} or *Hlf*^{+/+} littermate controls.
 (B) Time course of total donor contribution in PB 8 and 16 weeks post-transplantation.
 (C) Donor contribution in PB to each lineage 16 weeks post-transplant.
 (D) Lineage distribution in donor-derived PB of primary recipients 16 weeks post-transplantation.
 (E) Frequencies of total donor contribution and donor-derived LSK cells in BM of primary recipients 16 weeks post-transplantation (1°, primary BM transplantation, n = 6).
 (F) Total donor engraftment in secondary recipients and donor-derived LSK population (2°, secondary BM transplantation, n = 3).
 (G) Total donor engraftment in tertiary recipients (3°, tertiary BM transplantation, n = 3).
 (H) Competitive repopulation unit (CRU) frequency determined by ELDA (extreme limiting dilution analysis), showing the estimated HSC frequency (solid line) and confidence intervals (dotted lines) in the BM of *Hlf*^{-/-} or *Hlf*^{+/+} mice. n = 3–5 per genotype (3–4 recipients per donor at each cell concentration).
 (I) Schematic overview of the transplantation assay using isolated HSCs from *Hlf*^{-/-} or *Hlf*^{+/+} littermate controls.
 (J) Total donor contribution 16 weeks post-competitive transplantation using 50 purified HSCs (LSK CD34⁺ Flt3⁻) (n = 4).
 Data represent mean values (n > 3 per genotype). Error bars represent SEM. The asterisks indicate a significant difference (p).

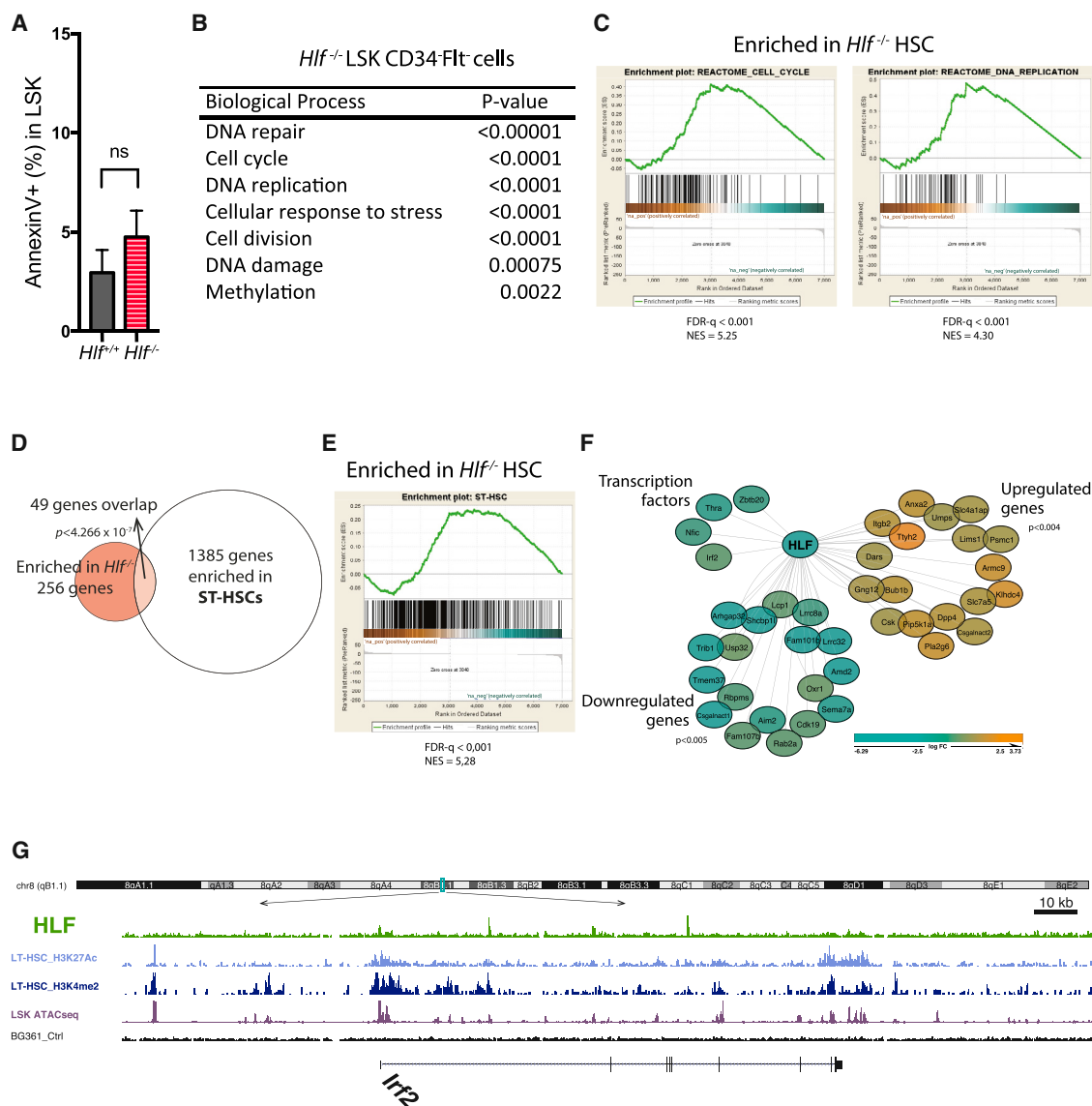


Figure 3. Gene Expression and CHIP-Seq Analysis Reveal that HLF Regulates HSC Cell-Cycle Activity

(A) Apoptosis levels in *Hlf*^{+/+} and *Hlf*^{-/-} LSK cells measured by Annexin-V staining (n = 3). Data represent mean values. Error bars represent SEM.

(B) Gene Ontology of the upregulated genes in *Hlf*^{-/-} HSCs (2-fold change $p < 0.05$). The transcriptome of purified HSCs (LSK CD34⁻ Flt3⁻) from *Hlf*^{-/-} mice was compared to *Hlf*^{+/+} control HSCs. See also Table S2.

(C) GSEA plots showing enrichment of upregulated genes in the *Hlf*^{-/-} HSC for cell cycle and DNA replication (n = 3).

(D) Venn diagram showing extensive overlap of genes between the significantly upregulated genes in *Hlf*^{-/-} HSCs in comparison to enriched genes in ST-HSCs (extracted from GEO: GSE9189).

(E) GSEA plots showing that *Hlf*^{-/-} HSCs are enriched for ST-HSC genes. The enrichment plot was obtained by adding the custom-made gene sets.

(F) Network showing the direct targets of HLF that were differentially expressed in *Hlf*^{-/-} HSCs (1.5-fold q value < 0.1).

(G) HLF-binding sites to the promoter of IRF2 correlated with active epigenetic marks.

HLF Deficiency Causes a Loss of HSC Quiescence

To functionally confirm findings from RNA and ChIP-seq, we performed cell-cycle analysis. These experiments revealed that while the majority (65.6%) of cells in the LSK CD34⁻ HSC population from *Hlf*^{+/+} mice were in G0 phase, substantially fewer (46.8%) of the corresponding *Hlf*^{-/-} cells were detected in this quiescent phase of the cell cycle. Accordingly, we observed a marked increase (43.6%) of *Hlf*^{-/-} LSK CD34⁻ cells residing in

the G1 phase compared to controls (27.1%) (Figures 4A and 4B). This demonstrates a relative loss of quiescence in *Hlf*^{-/-} HSCs. Notably, the change in the cell-cycle status was only detected in the HSC population (LSK CD34⁻) (Figure 4B), while the immediate downstream progenitors (LSK CD34⁺) were unaffected in comparison to controls (Figure 4C). To further support these data, cell-cycle analysis using bromodeoxyuridine (BrdU) staining also revealed an increased proportion of actively cycling

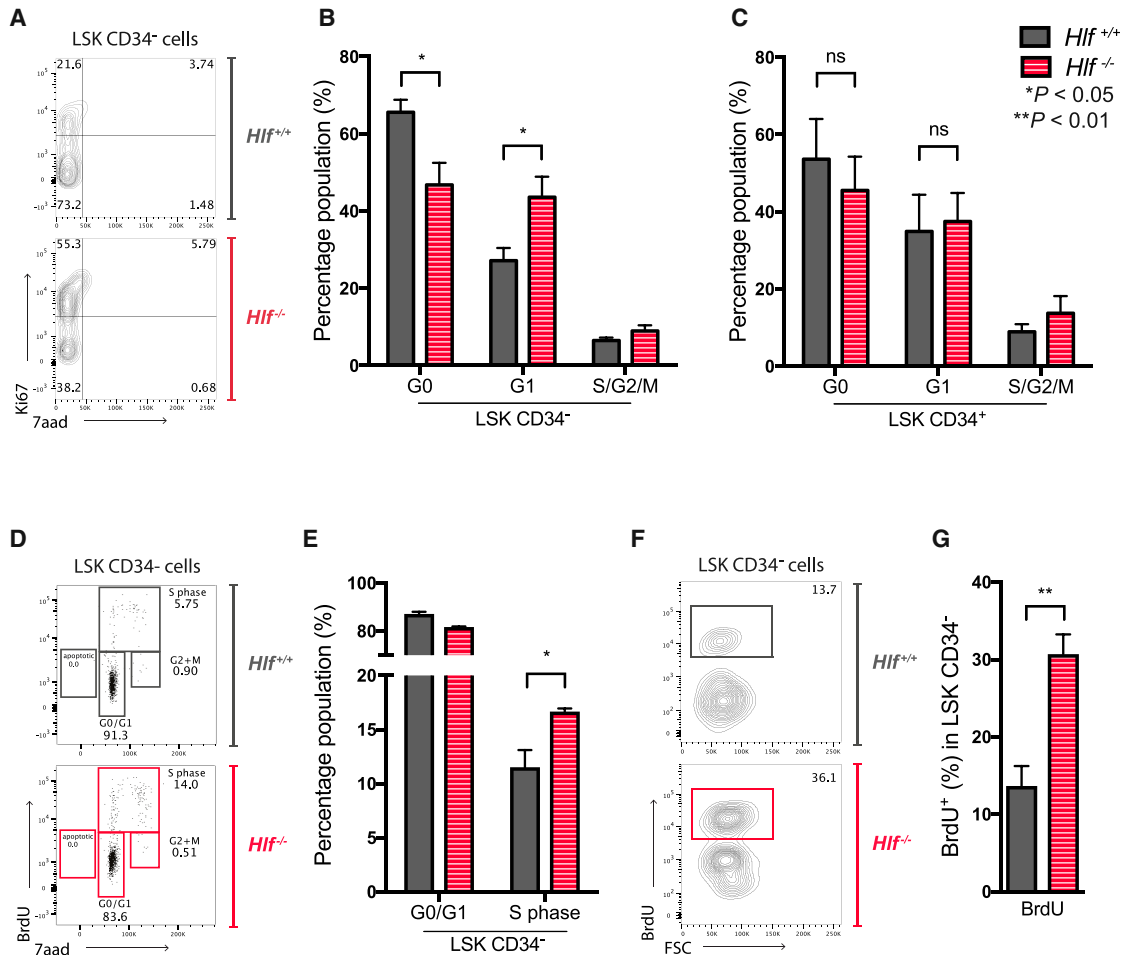


Figure 4. HLF Deficiency Causes a Loss of HSC Quiescence

(A) Representative FACS plots from cell-cycle analysis using Ki67 and 7-AAD of LSK CD34⁻ cells.

(B and C) Summary of the cell-cycle analysis of LSK CD34⁻ (B) and LSK CD34⁺ cells (C) in $Hif^{+/+}$ and $Hif^{-/-}$ BM at steady-state hematopoiesis (n = 9).

(D and E) Representative FACS plots of the cell-cycle kinetics of $Hif^{+/+}$ and $Hif^{-/-}$ LSK CD34⁻ cells at steady state using BrdU (D), and summary of FACS analysis (E) (n = 3).

(F and G) Representative FACS plots of incorporation of BrdU after daily BrdU intraperitoneal injection for 3 days (F), and summary of the analysis (G) (n = 4). Data represent mean values. Error bars represent SEM. Asterisks indicate a significant difference (p).

cells in the $Hif^{-/-}$ LSK CD34⁻ at steady-state hematopoiesis (Figures 4D and 4E). Next, to measure the rate of proliferating HSC *in vivo*, mice were treated with BrdU for 3 consecutive days. Significantly more LSK CD34⁻ cells incorporated BrdU in $Hif^{-/-}$ mice than in $Hif^{+/+}$ mice (Figures 4F and 4G), demonstrating that $Hif^{-/-}$ HSCs are more actively cycling than $Hif^{+/+}$ HSCs.

Interestingly, gene expression analysis revealed that CD48, which is normally expressed in less primitive and more activated hematopoietic progenitor cells (Kiel et al., 2005), was upregulated in $Hif^{-/-}$ HSCs (Table S1) and bound by HLF in ChIP-seq (Figure S2). Using flow cytometry, we confirmed that the LSK CD48⁻ CD150⁺ population was significantly reduced in the $Hif^{-/-}$ mice (Figures S3A and S3B) and that the majority of cells within the LSK CD34⁻ Flt3⁻ population from $Hif^{-/-}$ mice were positive for CD48 (Figures S3C and S3D). Additionally, no transplantable HSCs were detected in the LSK CD48⁻ CD150⁺ population (Fig-

ures S3E and S3F). These findings suggest that HLF may directly regulate the expression of CD48 or that the increased CD48 expression may reflect a more active state of $Hif^{-/-}$ HSCs. In addition, CD150 (Slamf7) was also among the HLF-bound genes identified in the ChIP-seq analysis (Figure S2), which could further contribute to the phenotypical shift of HSCs from the classical LSK CD48⁻ CD150⁺ population.

Taken together, the change in cell-cycle activity suggests that HLF is essential to maintain the quiescent state of HSCs under steady-state conditions *in vivo*.

HLF-Deficient HSCs Show Increased Sensitivity to Chemotoxic Insult and Irradiation

Our gene expression profiling and cell-cycle analysis indicated a more activated state of $Hif^{-/-}$ HSCs. We hypothesized that the loss of quiescence would make the $Hif^{-/-}$ HSCs more sensitive to toxic insults targeting dividing cells. To functionally test

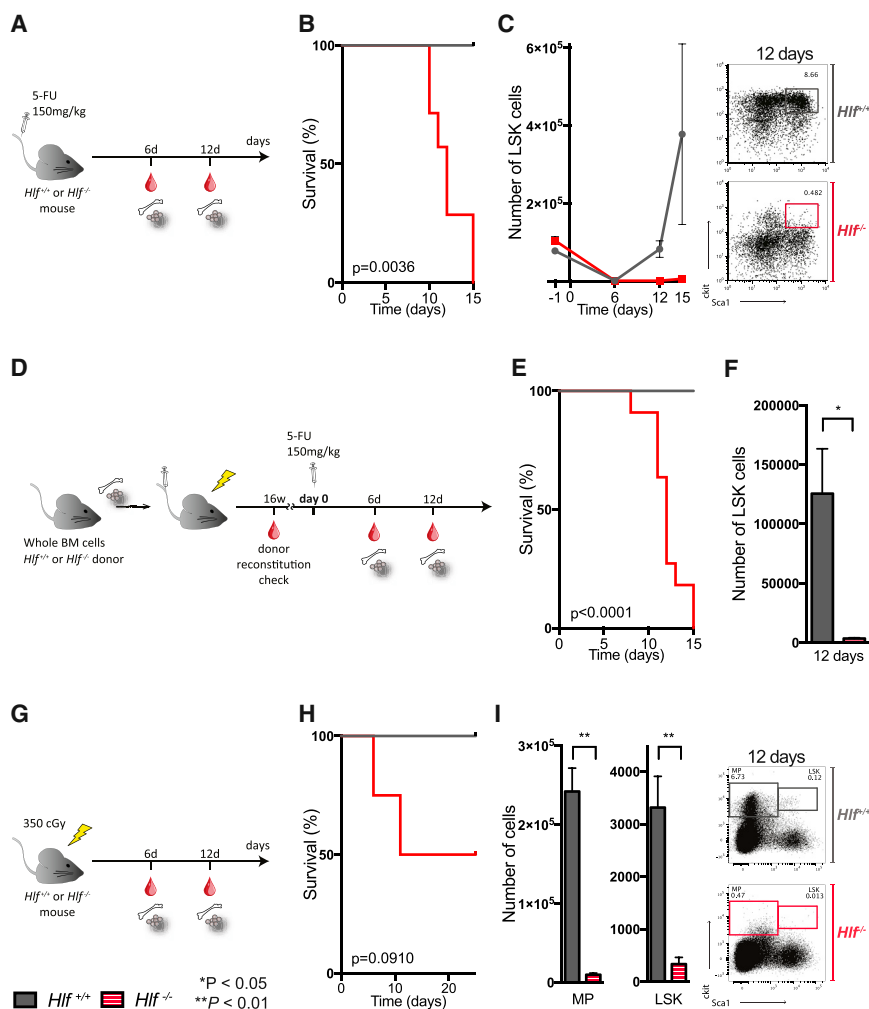


Figure 5. HLF-Deficient HSCs Show Increased Sensitivity to Chemotoxic Insult and Irradiation

(A) Schematic overview of the 5-FU treatment of steady-state mice. (B) Survival curve of *Hif*^{-/-} and *Hif*^{+/+} mice after a single dose of 5-FU administration (n = 8). (C) Absolute numbers of LSK cells in total BM 6, 12, and 15 days after 5-FU administration (left). Representative FACS plots of LSK cells from *Hif*^{+/+} and *Hif*^{-/-} mice 12 days after 5-FU treatment (right). See also Figure S4A. (D) Schematic overview of the 5-FU treatment done on previously transplanted mice and fully engrafted with donor cells. (E) Survival curve of mice fully reconstituted with *Hif*^{-/-} or *Hif*^{+/+} cells after a single dose of 5-FU administration (n = 11). (F) Absolute numbers of LSK cells in BM 12 days after 5-FU administration. See also Figure S4C. (G) Schematic overview of the experimental strategy for evaluating effects of sublethal irradiation. (H) Survival curve of *Hif*^{-/-} and *Hif*^{+/+} mice after sublethal irradiation (n = 4). (I) Numbers of multipotent progenitors (MPs; Lin⁻cKit⁺) and LSK cells in BM 12 days after sublethal irradiation, with representative FACS plots to the right (n = 7). See also Figure S4D. Data represent mean values. Error bars represent SEM. The asterisks indicate a significant difference (p).

Finally, since the PAR bZip family is known to regulate xenobiotic metabolism in hepatic cells (Gachon et al., 2006), we wondered whether the more severe BM failure induced by 5-FU treatment in the *Hif*^{-/-} mice was due to defective drug

this, we therefore studied the response of *Hif*^{-/-} HSCs to transient hematopoietic stress induced by the myeloablative agent 5-fluorouracil (5-FU), which preferentially eliminates actively cycling cells (Figure 5A). Strikingly, *Hif*^{-/-} mice receiving 5-FU were unable to recover from the severe myelosuppression induced by the drug, and none of these mice survived treatment (Figures 5B and S4A). This outcome was reflected in the BM profile by a complete loss of the LSK population that, unlike the situation in control animals, failed to recover (Figure 5C). To exclude the possibility that the increased sensitivity to 5-FU was influenced by toxicity to other, non-hematopoietic tissues, we transplanted *Hif*^{-/-} or *Hif*^{+/+} BM cells to irradiated wild-type (WT) recipient mice. First, we analyzed their blood parameters, which mirrored the levels seen at steady-state hematopoiesis (Figure S4B). Following complete BM reconstitution of donor cells, the mice were challenged by 5-FU treatment (Figure 5D). Mice reconstituted with *Hif*^{-/-} cells did not survive 5-FU treatment (Figures 5E and S4C) and showed a complete loss of the HSC compartment (Figure 5F), demonstrating that the increased sensitivity to 5-FU is indeed intrinsic to hematopoietic cells.

metabolism. To address this, we used sublethal irradiation as an alternative, non-pharmacological, toxic insult to target dividing cells (Figure 5G). Similar to 5-FU treatment, *Hif*^{-/-} mice showed significantly lower survival after exposure to sublethal irradiation (Figures 5H and S4D). Moreover, 12 days post-irradiation, *Hif*^{-/-} mice displayed a dramatic reduction of hematopoietic progenitor cells compared to control mice (Figure 5I). Taken together, these results strongly imply that HLF is crucial for protecting HSCs from toxic insults by preserving their quiescent state.

DISCUSSION

HLF has been suggested as an important regulator of HSC function when ectopically expressed, but until now, the physiological role of HLF in HSC biology has remained unknown. Here, using HLF knockout mice, we demonstrate that HLF is essentially dispensable for hematopoiesis under steady-state conditions. However, HLF-deficient HSCs were found to reside in a more “active” (less quiescent) state, both transcriptionally and functionally, and upon serial transplantation showed reduced

reconstitution capacity and impaired self-renewal potential. Moreover, HLF-deficient mice demonstrated an increased sensitivity to treatment with cytotoxic drugs and sublethal irradiation, which eradicated the hematopoietic stem/progenitor cell pool and severely reduced the survival of *Hlf*^{-/-} mice. In addition, CD48 and CD150 were identified as direct targets of HLF. In accordance with this, no HSCs were present within the classical LSK CD48⁺CD150⁻ population in *Hlf*^{-/-} mice, even though the HSC pool size was not altered.

Our findings strongly suggest that HLF is an essential regulator of HSC quiescence and that HLF deficiency leads to an exhaustion of HSCs in adult mouse BM during regeneration or following cytotoxic stress. In line with this, genome-wide expression analysis of *Hlf*^{-/-} HSCs overlapped with ChIP-seq analysis not only revealed general patterns associated with increased cell cycling and activation but also identified a number of known HSC regulators (some directly bound by HLF) that were significantly altered and that may provide further mechanistic insight into the enhanced cell-cycle progression. For example, the transcriptional repressors GF11 and IRF2, whose deficiency has been reported to result in HSC exhaustion due to loss of HSC quiescence in adult hematopoiesis (Hock et al., 2004; Sato et al., 2009; Zeng et al., 2004), were found to be downregulated in *Hlf*^{-/-} HSCs, akin to the *Hlf*^{-/-} phenotype. Interestingly, GF11 has been shown to be regulated by LMO2 (Cheng et al., 2016), which is a known target gene of the E2A-HLF fusion protein (de Boer et al., 2011; Yamada et al., 1998). These findings indicate a potential regulatory axis linking HLF, GF11, and LMO2, and it would be interesting to further study the connection between LMO2 and GF11 in *Hlf*^{-/-} HSCs.

In addition, we found that HLF binds to the promotor of IRF2 and that the binding site was surrounded by active histone marks, indicating that HLF promotes the expression of *Irf2* in HSCs. This is in line with the significant reduction in gene expression of *Irf2* detected in *Hlf*^{-/-} HSCs. Given its important role in HSC regulation, *Irf2* could be a major contributor to the loss of HSC quiescence detected in *Hlf*^{-/-} mice. In fact, *Irf2*^{-/-} HSCs were found to be highly proliferative and failed to engraft in competitive repopulation assays (Sato et al., 2009). Interestingly, IRF2 is known to suppress interferon (IFN) signaling, which is elevated during stress, and strikingly, it was shown that HSC function in *Irf2*^{-/-} mice was restored by disabling IFN signaling (Baldrige et al., 2010; Brzostek-Racine et al., 2011; Sato et al., 2009). These data suggest that HLF may protect HSCs from exhaustion triggered by stress responses from the immune system.

In an alternative scenario, HLF may be directly involved in structuring the HSC-specific gene network, with the reduced quiescence being a result of the loss of stem cell potential. While this would, in a traditional view, argue that HLF-deficient mice are unable to sustain normal hematopoiesis long-term, recent studies have suggested that HSCs may have limited contribution to adult steady-state hematopoiesis (Busch et al., 2015; Sun et al., 2014), with only marginal effects on hematopoiesis observed even upon severe and irreversible HSC depletion (Schoedel et al., 2016). A potential loss in stem cell potency in the HLF-deficient setting may therefore be compatible with normal steady-state hematopoiesis and only become evident during immediate settings of regeneration or toxic stress. This

correlates with the downregulation of HLF during normal HSC differentiation (Gazit et al., 2013) and to the decline of HLF upon *in vitro* culture (Magnusson et al., 2013), events that are both connected to compromised stem cell activity. Reciprocally, enforced expression of HLF in both mouse and human HSCs prolonged their *in vitro* self-renewal capacity (Gazit et al., 2013; Calvanese et al., 2014), with an essential contribution of HLF for successful *in vivo* reprogramming of B cells into induced HSCs (iHSCs) (Riddell et al., 2014), further implying a critical role of HLF in the gene regulatory networks governing HSC fate options.

In conclusion, we link the primary hematopoietic phenotype of HLF knockout mice directly to HSCs, in accordance with the unique expression pattern of HLF in hematopoiesis. Thus, HLF appears to be primarily required for HSC integrity in adult hematopoiesis. In this manner, HLF provides an important entry point in unraveling the molecular mechanisms regulating HSC identity and quiescence.

EXPERIMENTAL PROCEDURES

Mice

C57BL/6 (CD45.2), B6SJL (CD45.1), and C57BL/6 × B6SJL (CD45.1/CD45.2) mice were maintained in individually ventilated racks and given autoclaved food and water *ad libitum*. The generation of the *Hlf*^{-/-} mice (obtained from the European Mouse Mutant Archive) was previously described (Gachon et al., 2004), and mice were backcrossed to C57BL/6 on-site. All experiments were performed using mice at 9–16 weeks of age of any gender. All mice were maintained according to Swedish animal guidelines at the Lund University animal facility, and all animal experiments were performed with consent from the local ethical committee (ethical permit M94-15).

Real-Time qPCR

Total RNA was isolated from fluorescence-activated cell sorting (FACS)-sorted cells using the RNeasy micro kit (QIAGEN) and reverse transcribed (SuperScript III, Invitrogen) in the presence of random hexamers. Real-time PCRs were performed on 7900HT Fast Real Time PCR system (Applied Biosystems) according to the manufacturer's protocol with gene-specific primers (Applied Biosystems) and SDS 2.2.1 software. Each assay was performed in triplicate, and the results were normalized to the housekeeping gene hypoxanthine guanine phosphoribosyl transferase (*Hprt*).

PB and Bone Marrow Preparation

PB was collected from the tail vein using microvette tubes (Sarstedt) and kept in heparin (2,000 IU/mL; Leo Pharma). Blood parameters were analyzed using SysmexXE-5000 (Sysmex Europoe). Before antibody staining of the PB, erythrocytes were lysed twice with 150 mM ammonium chloride (NH₄Cl; STEMCELL Technologies) for 10 min at room temperature. Bone marrow (BM) cells were isolated by crushing femur and tibia from each mouse in PBS containing 2% fetal calf serum (FCS) (Gibco). Cells were passed through a nylon filter (70 μm; BD Biosciences) to obtain single-cell suspensions.

Flow Cytometry Analysis

For lineage analysis, cells were stained with the combinations of fluorochrome-conjugated monoclonal antibodies for cell-surface markers for 30 min in darkness on ice. For stem and progenitor cell sorting purposes, BM cells were lineage depleted using anti-lineage microbeads with the MACS separation column (Miltenyi Biotec) according to manufacturer protocol, followed by staining with the combinations of fluorochrome-conjugated monoclonal antibodies. 7-Aminoactinomycin D (7-AAD; Invitrogen) or propidium iodide (Invitrogen) was used to exclude dead cells. All experiments were performed using FACS Canto, FACS LSR II cytometers, FACS Aria III, or FACS Aria III cell sorters (Becton Dickinson) and analyzed by FlowJo software (Tree Star, version 9.5.1 or 10.0.2). Antibodies used in analyses are listed in Table S4.

Competitive Transplantation Assay

For total BM cell transplantation, 2×10^5 unfractionated BM cells from *Hlf*^{+/+} or *Hlf*^{-/-} BM donors (CD45.2) and competitor cells (CD45.1) were mixed in a 1:1 ratio, and then intravenously injected to lethally irradiated (900 cGy) recipient mice (CD45.1/CD45.2). For HSC transplantations, 50 purified LSK CD34⁻Flt3⁻ cells were sorted from *Hlf*^{+/+} or *Hlf*^{-/-} BM cells (CD45.2) and mixed with 2×10^5 unfractionated BM support cells (CD45.1) and transplanted into lethally irradiated (900 cGy) recipient mice (CD45.1/CD45.2). PB was collected and analyzed every 4 weeks. After 16 weeks, the engrafted mice were sacrificed and the BM cells were harvested and subjected to further functional and phenotypic analyses.

The competitive repopulating cell frequency was determined using 1×10^5 , 5×10^4 , 1×10^4 , and 5×10^3 unfractionated BM cells in competition to 2×10^5 competitor cells. The cell dose was considered to contain at least one CRU if donor engraftment in the BM exceeded 1% of both lymphoid and myeloid lineages. The CRU frequency was calculated and plotted using extreme limiting dilution analysis (ELDA) as previously described (Hu and Smyth, 2009).

Apoptosis Assay

BM cells prestained for HSC markers were stained with phycoerythrin (PE)-conjugated Annexin-V and 7-AAD (BD Biosciences) according to the manufacturer's protocol. Annexin-V binding and 7-AAD incorporation were measured using FACS Canto II.

Cell-Cycle and Cell Proliferation Analysis

For *in vitro* cell-cycle analysis, the PE Mouse Anti-Ki-67 Set (BD Biosciences) was used. Fresh BM cells were stained with the antibody cocktail for the HSC fraction. Cells were then fixed and permeabilized using the BD Cytotfix Cytoperm Fixation kit (BD Biosciences) and stained with anti-Ki67 according to the manufacturer's protocol. Cells were analyzed for Ki67 expression and 7-AAD incorporation using flow cytometry.

For *in vivo* cell-cycle analysis with BrdU, the APC BrdU Flow kit (BD Pharmingen) was used. Mice received a single intraperitoneal injection of 1 mg BrdU per recipient. After 1 hr, mice were euthanized, and BM cells were stained with antibody cocktail for the HSC fraction, fixed and permeabilized according to the manufacturer's protocol, and analyzed by flow cytometry.

For *in vivo* labeling with BrdU, mice were intraperitoneally injected with 1 mg BrdU per mouse for 3 days and then euthanized 3 hr after the last injection. BM cells were prepared according to the manufacturer's protocol and analyzed by flow cytometry.

5-FU Treatment and Sublethal Irradiation

Steady-state mice or fully reconstituted mice (16 weeks post-transplantation) transplanted with either *Hlf*^{+/+} or *Hlf*^{-/-} BM cells were intravenously injected once with 5-FU (APP Pharmaceuticals) at 150 mg/kg body weight. To give a sublethal dose of radiation, the mice were irradiated with 350 cGy total body radiation.

RNA-Seq and ChIP-Seq Analyses

Total RNA was isolated from 3,000 sorted LSK CD34⁻Flt3⁻ cells using the QIAshredder and RNeasy Mini Kit (QIAGEN). RNA libraries were constructed by the UCLA Clinical Microarray Core, Los Angeles, using TruSeq kits (Illumina). The RNA libraries were sequenced on a HiSeq 2000/2500 at 2 × 100 bp. Transcript levels were estimated using the method RSEM (RNA-seq by expectation maximization) (Li and Dewey, 2011). Reads were mapped using bowtie2 method to the mouse RefSeq transcripts obtained from University of California, Santa Cruz (UCSC) (Speir et al., 2016). Pairwise differential expression assessments were performed using the method EBSeq (Leng et al., 2013); genes were considered to be differentially expressed based on a false discovery rate of less than 5% (posterior probability of being differentially expressed < 0.05). GO analysis was performed using DAVID. GSEA was performed using the method GSEA Preranked. All p and false discovery rate (FDR) q values were calculated as described previously (Mootha et al., 2003). Ranked lists of genes with a fold change of greater than 1.5 were used as input for GSEA preranked. The enrichment plots were obtained using curated gene sets in GSEA MSigDB and were obtained by adding the costume made gene sets (generated from GEO: GSE9189 by comparing LT-HSC and ST-HSC p < 0.01 and fold-change threshold of 2 as a filter) to the curated

gene sets in GSEA MSigDB. ChIP-seq was performed as described previously (Wahlestedt et al., 2017). Briefly, peak regions were called using MACS2 (Zhang et al., 2008) and density plots generated in bigwig format. These were then displayed together as custom tracks on the UCSC Genome Browser. Peaks were assigned to genes if the peak was (1) in a promoter according to MPromDB (Gupta et al., 2011), (2) not in a promoter but intragenic, or (3) neither in a promoter nor intragenic but intergenic within 50 kb from the start or end of a gene. Motif discovery was performed using the HOMER program (Heinz et al., 2010). The HLF-bound genes identified in ChIP-seq were used to generate the HLF network in Cytoscape 3.0.0. To explore the gene expression status of HLF-bound targets, we overlaid the RNA-seq data derived from *Hlf*^{-/-} mice. Differentially expressed genes (with p values < 0.1) were also overlaid with the HLF network to identify the enriched targets. To visualize genome data, we used the UCSC Genome Browser.

Statistical Analyses

Graphs were generated using GraphPad (Prism Version 7 software). Mann-Whitney or Student's t test was used to determine statistical significance, and 2-tailed p values are shown (significance levels: *p < 0.05, **p < 0.01, ***p < 0.001, ****p < 0.0001). All error bars represent SEM.

DATA AND SOFTWARE AVAILABILITY

The accession numbers for the RNA-seq and ChIP-seq data reported in this study are GEO: GSE100385 and GEO: GSE69817 (Wahlestedt et al., 2017), respectively.

SUPPLEMENTAL INFORMATION

Supplemental Information includes Supplemental Experimental Procedures, four figures, and four tables and can be found with this article online at <https://doi.org/10.1016/j.celrep.2017.11.084>.

ACKNOWLEDGMENTS

The authors thank the staff at BMC for excellent animal care, as well as the Lund Stem Cell FACS Core Facilities for assistance with cell sorting. The authors also thank Frédéric Gachon for helping with obtaining the *Hlf*^{-/-} mice. This work was supported by the Swedish Cancer Foundation CAN 2011/873, CAN 2014/914 (to M.M.), the Swedish Research Council 521-2011-2905 (to M.M.), the Swedish Child Cancer Foundation PR12/097, PR2015-0070 (to M.M.), and the Swedish Society for Medical Research (to M.M.).

AUTHORSHIP CONTRIBUTIONS

K.K. designed and performed experiments, analyzed data, and wrote the manuscript. A.D., M.W., S.D., and J.C. helped perform several experiments. A.S. helped visualize RNA-seq and ChIP-seq overlap. S.S. and B.V.H. helped analyze RNA-seq data. H.K.A.M., K.M., D.B., and J.L. helped analyze experiments and edited the manuscript. M.M. designed and supervised the research and wrote the manuscript.

DECLARATION OF INTERESTS

The authors declare no competing interests.

Received: June 27, 2017

Revised: October 19, 2017

Accepted: November 22, 2017

Published: December 19, 2017

REFERENCES

Baldrige, M.T., King, K.Y., Boles, N.C., Weksberg, D.C., and Goodell, M.A. (2010). Quiescent haematopoietic stem cells are activated by IFN-gamma in response to chronic infection. *Nature* 465, 793–797.

- Bryder, D., Rossi, D.J., and Weissman, I.L. (2006). Hematopoietic stem cells: the paradigmatic tissue-specific stem cell. *Am. J. Pathol.* *169*, 338–346.
- Brzostek-Racine, S., Gordon, C., Van Scoy, S., and Reich, N.C. (2011). The DNA damage response induces IFN. *J. Immunol.* *187*, 5336–5345.
- Busch, K., Klapproth, K., Barile, M., Flossdorf, M., Holland-Letz, T., Schlenner, S.M., Reth, M., Höfer, T., and Rodewald, H.R. (2015). Fundamental properties of unperturbed haematopoiesis from stem cells in vivo. *Nature* *518*, 542–546.
- Cheng, H., Ang, H.Y., A El Farran, C., Li, P., Fang, H.T., Liu, T.M., Kong, S.L., Chin, M.L., Ling, W.Y., Lim, E.K., et al. (2016). Reprogramming mouse fibroblasts into engraftable myeloerythroid and lymphoid progenitors. *Nat. Commun.* *7*, 13396.
- de Boer, J., Yeung, J., Ellu, J., Ramanujachar, R., Bornhauser, B., Solarska, O., Hubank, M., Williams, O., and Brady, H.J. (2011). The E2A-HLF oncogenic fusion protein acts through Lmo2 and Bcl-2 to immortalize hematopoietic progenitors. *Leukemia* *25*, 321–330.
- Dorn, D.C., Kou, C.A., Png, K.J., and Moore, M.A. (2009). The effect of cantharidins on leukemic stem cells. *Int. J. Cancer* *124*, 2186–2199.
- Eliasson, P., and Jönsson, J.I. (2010). The hematopoietic stem cell niche: low in oxygen but a nice place to be. *J. Cell. Physiol.* *222*, 17–22.
- Ficara, F., Murphy, M.J., Lin, M., and Cleary, M.L. (2008). Pbx1 regulates self-renewal of long-term hematopoietic stem cells by maintaining their quiescence. *Cell Stem Cell* *2*, 484–496.
- Gachon, F., Fonjallaz, P., Damiola, F., Gos, P., Kodama, T., Zakany, J., Duboule, D., Petit, B., Tafti, M., and Schibler, U. (2004). The loss of circadian PAR bZip transcription factors results in epilepsy. *Genes Dev.* *18*, 1397–1412.
- Gachon, F., Olela, F.F., Schaad, O., Descombes, P., and Schibler, U. (2006). The circadian PAR-domain basic leucine zipper transcription factors DBP, TEF, and HLF modulate basal and inducible xenobiotic detoxification. *Cell Metab.* *4*, 25–36.
- Gazit, R., Garrison, B.S., Rao, T.N., Shay, T., Costello, J., Ericson, J., Kim, F., Collins, J.J., Regev, A., Wagers, A.J., and Rossi, D.J.; Immunological Genome Project Consortium (2013). Transcriptome analysis identifies regulators of hematopoietic stem and progenitor cells. *Stem Cell Reports* *1*, 266–280.
- Gupta, R., Bhattacharyya, A., Agosto-Perez, F.J., Wickramasinghe, P., and Davuluri, R.V. (2011). MPromDb update 2010: an integrated resource for annotation and visualization of mammalian gene promoters and ChIP-seq experimental data. *Nucleic Acids Res.* *39*, D92–D97.
- Heinz, S., Benner, C., Spann, N., Bertolino, E., Lin, Y.C., Laslo, P., Cheng, J.X., Murre, C., Singh, H., and Glass, C.K. (2010). Simple combinations of lineage-determining transcription factors prime cis-regulatory elements required for macrophage and B cell identities. *Mol. Cell* *38*, 576–589.
- Hock, H., Hamblen, M.J., Rooke, H.M., Schindler, J.W., Saleque, S., Fujiwara, Y., and Orkin, S.H. (2004). Gfi-1 restricts proliferation and preserves functional integrity of haematopoietic stem cells. *Nature* *431*, 1002–1007.
- Hu, Y., and Smyth, G.K. (2009). ELDA: extreme limiting dilution analysis for comparing depleted and enriched populations in stem cell and other assays. *J. Immunol. Methods* *347*, 70–78.
- Hunger, S.P., Ohyashiki, K., Toyama, K., and Cleary, M.L. (1992). Hlf, a novel hepatic bZIP protein, shows altered DNA-binding properties following fusion to E2A in t(17;19) acute lymphoblastic leukemia. *Genes Dev.* *6*, 1608–1620.
- Inaba, T., Roberts, W.M., Shapiro, L.H., Jolly, K.W., Raimondi, S.C., Smith, S.D., and Look, A.T. (1992). Fusion of the leucine zipper gene HLF to the E2A gene in human acute B-lineage leukemia. *Science* *257*, 531–534.
- Inukai, T., Hirose, K., Inaba, T., Kurosawa, H., Hama, A., Inada, H., Chin, M., Nagatoshi, Y., Ohtsuka, Y., Oda, M., et al. (2007). Hypercalcemia in childhood acute lymphoblastic leukemia: frequent implication of parathyroid hormone-related peptide and E2A-HLF from translocation 17;19. *Leukemia* *21*, 288–296.
- Ivanova, N.B., Dimos, J.T., Schaniel, C., Hackney, J.A., Moore, K.A., and Lemischka, I.R. (2002). A stem cell molecular signature. *Science* *298*, 601–604.
- Kiel, M.J., Yilmaz, O.H., Iwashita, T., Yilmaz, O.H., Terhorst, C., and Morrison, S.J. (2005). SLAM family receptors distinguish hematopoietic stem and progenitor cells and reveal endothelial niches for stem cells. *Cell* *121*, 1109–1121.
- Leng, N., Dawson, J.A., Thomson, J.A., Ruotti, V., Rissman, A.I., Smits, B.M., Haag, J.D., Gould, M.N., Stewart, R.M., and Kendziorski, C. (2013). EBSeq: an empirical Bayes hierarchical model for inference in RNA-seq experiments. *Bioinformatics* *29*, 1035–1043.
- Li, B., and Dewey, C.N. (2011). RSEM: accurate transcript quantification from RNA-Seq data with or without a reference genome. *BMC Bioinformatics* *12*, 323.
- Magnusson, M., Sierra, M.I., Sasidharan, R., Prashad, S.L., Romero, M., Saarikoski, P., Van Handel, B., Huang, A., Li, X., and Mikkola, H.K. (2013). Expansion on stromal cells preserves the undifferentiated state of human hematopoietic stem cells despite compromised reconstitution ability. *PLoS ONE* *8*, e53912.
- Moore, M.A., Dorn, D.C., Schuringa, J.J., Chung, K.Y., and Morrone, G. (2007). Constitutive activation of Flt3 and STAT5A enhances self-renewal and alters differentiation of hematopoietic stem cells. *Exp. Hematol.* *35* (4, Suppl 1), 105–116.
- Mootha, V.K., Lindgren, C.M., Eriksson, K.F., Subramanian, A., Sihag, S., Lehar, J., Puigserver, P., Carlsson, E., Ridderstråle, M., Laurila, E., et al. (2003). PGC-1alpha-responsive genes involved in oxidative phosphorylation are coordinately downregulated in human diabetes. *Nat. Genet.* *34*, 267–273.
- Orkin, S.H., and Zon, L.I. (2008). Hematopoiesis: an evolving paradigm for stem cell biology. *Cell* *132*, 631–644.
- Riddell, J., Gazit, R., Garrison, B.S., Guo, G., Saadatpour, A., Mandal, P.K., Ebina, W., Volchkov, P., Yuan, G.C., Orkin, S.H., and Rossi, D.J. (2014). Reprogramming committed murine blood cells to induced hematopoietic stem cells with defined factors. *Cell* *157*, 549–564.
- Sato, T., Onai, N., Yoshihara, H., Arai, F., Suda, T., and Ohteki, T. (2009). Interferon regulatory factor-2 protects quiescent hematopoietic stem cells from type I interferon-dependent exhaustion. *Nat. Med.* *15*, 696–700.
- Schoedel, K.B., Morcos, M.N.F., Zerjatke, T., Roeder, I., Grinenko, T., Voehringer, D., Göthert, J.R., Waskow, C., Roers, A., and Gerbaulet, A. (2016). The bulk of the hematopoietic stem cell population is dispensable for murine steady-state and stress hematopoiesis. *Blood* *128*, 2285–2296.
- Shojaei, F., Trowbridge, J., Gallacher, L., Yuefei, L., Goodale, D., Karanu, F., Levac, K., and Bhatia, M. (2005). Hierarchical and ontogenic positions serve to define the molecular basis of human hematopoietic stem cell behavior. *Dev. Cell* *8*, 651–663.
- Speir, M.L., Zweig, A.S., Rosenbloom, K.R., Raney, B.J., Paten, B., Nejad, P., Lee, B.T., Learned, K., Karolchik, D., Hinrichs, A.S., et al. (2016). The UCSC Genome Browser database: 2016 update. *Nucleic Acids Res.* *44* (D1), D717–D725.
- Sun, J., Ramos, A., Chapman, B., Johnnidis, J.B., Le, L., Ho, Y.J., Klein, A., Hofmann, O., and Camargo, F.D. (2014). Clonal dynamics of native haematopoiesis. *Nature* *514*, 322–327.
- Calvanese, V., Prashad, S.L., Magnusson, M., and Mikkola, H.K.A. (2014). Analysis of highly self-renewing GPI-80+ human fetal hematopoietic stem cells identifies novel regulators of stemness. *Blood* *124*, 4314.
- Wahlestedt, M., Ladopoulos, V., Hidalgo, I., Sanchez Castillo, M., Hannah, R., Säwén, P., Wan, H., Dudenhöffer-Pfeifer, M., Magnusson, M., Norddahl, G.L., et al. (2017). Critical modulation of hematopoietic lineage fate by hepatic leukemia factor. *Cell Rep* *21*, 2251–2263.
- Waters, K.M., Sontag, R.L., and Weber, T.J. (2013). Hepatic leukemia factor promotes resistance to cell death: implications for therapeutics and chronotherapy. *Toxicol. Appl. Pharmacol.* *268*, 141–148.
- Weissman, I.L. (2000). Stem cells: units of development, units of regeneration, and units in evolution. *Cell* *100*, 157–168.
- Yamada, Y., Warren, A.J., Dobson, C., Forster, A., Pannell, R., and Rabbits, T.H. (1998). The T cell leukemia LIM protein Lmo2 is necessary for adult mouse hematopoiesis. *Proc. Natl. Acad. Sci. USA* *95*, 3890–3895.
- Zeng, H., Yücel, R., Kosan, C., Klein-Hitpass, L., and Möröy, T. (2004). Transcription factor Gfi1 regulates self-renewal and engraftment of hematopoietic stem cells. *EMBO J.* *23*, 4116–4125.
- Zhang, Y., Liu, T., Meyer, C.A., Eeckhoutte, J., Johnson, D.S., Bernstein, B.E., Nusbaum, C., Myers, R.M., Brown, M., Li, W., and Liu, X.S. (2008). Model-based analysis of ChIP-seq (MACS). *Genome Biol.* *9*, R137.